

Diffusion tensor imaging in the differentiation of adrenal adenomas and metastases

Yüksel Işık, Bengi Gürses, Neslihan Taşdelen, Özgür Kılıçkesmez, Zeynep Fırat, Çetin Ordu, Nevzat Gürmen

PURPOSE

To determine the utility of diffusion tensor imaging for the differentiation of adrenal adenomas and metastases.

MATERIALS AND METHODS

Thirty-three patients with a mean age of 59 years were included in this study. Each subject presented with a single adrenal lesion (19 adenomas, 14 metastases). Magnetic resonance imaging (MRI) was performed in the coronal plane using a 3 Tesla MRI and a six-channel phased array SENSE torso coil. T1-weighted in-phase and opposed-phase, T2-weighted turbo spin-echo, and single-shot echo-planar diffusion tensor imaging (DTI) sequences were used for image acquisition. To determine apparent diffusion coefficients (ADC) and fractional anisotropy (FA) values of adrenal lesions, coronal T2-weighted images were used as anatomical references and to localize regions of interest on DTI images. The signal intensity (SI) indices were obtained from in-phase/opposed-phase images by a radiologist blinded to the DTI findings. The DTI parameters were determined by a different radiologist. The SI indices and the differences in FA and ADCs between adenomas and metastases were compared. Analyses of receiver operating characteristics (ROC) were performed to determine the area under the curve (AUC).

RESULTS

The SI index of adenomas was found to be significantly higher than the value determined for metastases. Moreover, the median FA value of adrenal adenomas was found to be significantly higher than that of metastases. No statistically significant difference was observed in the ADCs between adenomas and metastases. Furthermore, no significant correlation was found among the SI index and the measured DTI parameters. Based on ROC analyses, the AUC was found to be 0.936 in FA measurements with a 95% confidence interval. The cut-off value obtained from this analysis was 0.40 with maximum sensitivity and specificity values of 74% and 88%, respectively.

CONCLUSION

Although no significant difference was observed in the ADCs between adrenal adenomas and metastases, the FA values differed significantly. The FA values may have the potential to differentiate between adrenal adenomas and metastases, which is a possibility that should be validated by further research.

Key words: • adrenal glands • diffusion tensor imaging • adenoma

Most adrenal lesions are discovered during radiological examinations performed for unrelated reasons (1). Differentiating adenomas from metastases has been the major objective in the radiological evaluation of adrenal masses, especially in patients with a known primary malignancy. For oncologic patients, the precise identification of adrenal metastases is crucial for staging of the disease and for deciding upon a treatment strategy (1, 2).

Various imaging modalities have been investigated for their ability to characterize adrenal lesions. In the context of lipid-rich adenomas, the detection of lipid content with unenhanced computed tomography (CT) and magnetic resonance imaging (MRI) using a chemical shift technique allows for correct diagnoses in most instances (1–3). Furthermore, low-density (Hounsfield unit) values are characteristically observed on CT images. Furthermore, signal loss is common when using opposed-phase (OP) MRI compared with in-phase (IP) imaging. Characteristic enhancement patterns are frequently used to identify lipid-rich adenomas. Drawing a clear distinction between metastases and adenomas, however, is not always possible, especially for lipid-poor adenomas (1–3). Numerous studies have evaluated the efficiency of positron emission CT (PET-CT) in differentiating benign and malignant adrenal lesions. Although this technique is reported to have high sensitivity and specificity, it is well known that a subset of adenomas demonstrates slightly increased uptake, and a subset of metastatic lesions may not demonstrate any uptake (1–4).

The primary aim in imaging adrenal lesions is to non-invasively differentiate adenomas from metastases. In recent years, the role of diffusion-weighted imaging (DWI) in the evaluation of adrenal lesions has been investigated (5). DWI is well known to provide valuable qualitative and quantitative data regarding the cellularity and cell membrane integrity in various tissues based on measurements of Brownian motion (6). The role of DWI has been investigated in a variety of tumors, and significant differences in apparent diffusion coefficients (ADC) were detected between tumoral and non-tumoral tissues (5–7). With the help of the echo planar imaging (EPI) and parallel imaging technology, DWI has also been applied with acceptable resolution and acquisition times to the abdominal viscera (6). The role of DWI has been investigated in various intra-abdominal viscera, including the genital organs, liver, kidneys, pancreas, and other regions of the gastrointestinal tract (6–10). There are a limited number of studies that use DWI to examine the adrenal glands, and most of these studies suggest that there is no significant difference in the ADCs of benign and malignant adrenal lesions (5, 11). Diffusion tensor imaging (DTI) allows the analysis of water diffusion in at least six directions and, therefore, aids in the evaluation of the anisotropic properties of various tissues (12). DTI has also been applied

From the Departments of Radiology (Y.I., B.G. ✉ bengur0@yahoo.com, N.T., Ö.K., Z.F., N.G.) and Internal Medicine and Oncology (Ç.O.), Yeditepe University School of Medicine, İstanbul, Turkey.

Received 7 May 2011; revision requested 12 June 2011; revision received 20 June 2011; accepted 27 June 2011.

Published online 30 September 2011
DOI 10.4261/1305-3825.DIR.4582-11.1

to analyses of the abdominal viscera in recent years. To the best of our knowledge, however, there are no published studies of the adrenal system that make use of DTI (12).

Three-Tesla (3 T) MRI systems provide an enhanced signal-to-noise ratio and, therefore, a better resolution for DWI and DTI techniques. The increased susceptibility artifact, which is a major drawback of high-power magnetic field systems, is overcome with the aid of parallel imaging technology (12). In this study, the role of DTI in the differentiation of adrenal adenomas and metastases was investigated using 3 T MRI and parallel imaging technology.

Materials and methods

Study population

In total, 33 patients were included in the study. These patients presented with a total of 33 adrenal lesions (19 adenoma and 14 metastases, no bilateral lesions), which were detected using different radiologic modalities in our department between June and August 2010. Informed consent was obtained from each patient prior to the study. Lesions less than 1 cm in diameter were not included, given that the fractional anisotropy (FA) and ADC measurements would not be precise. The mean patient age was 59 years (range, 18–80 years). Twenty-seven patients were male and six were female. For cases of adenoma, a definitive diagnosis was reached using standard imaging and/or a finding of no change in lesion size for six months. For cases of adrenal metastases, a definitive diagnosis was determined based on histopathological findings or an increased lesion size upon follow-up. All patients with adrenal metastases had a primary diagnosis of lung cancer.

MRI

The study was approved by the local ethics committee, and informed consent was obtained from each subject prior to the MRI examination. Each MRI examination was performed with a 3 T scanner (Intera Achieva, Philips, Best, The Netherlands) equipped with a six-channel phased array SENSE Torso coil high-performance gradients with a maximum strength of 80 mT/m and a slew rate of 200 mT/m/ms. In all patients, coronal T1-weighted IP (TR, 10 ms; TE, 2.3 ms; slice thickness,

3 mm; slice gap, 0 mm; flip angle, 15°; acquisition time, 36 s), OP (TR, 10 ms; TE, 1.3 ms; slice thickness, 3 mm; slice gap, 0 mm; flip angle, 15°; acquisition time, 36 s), coronal T2 turbo spin echo (TSE) (TR, 2046 ms; TE, 68 ms; matrix, 100×127, slice thickness, 3 mm; slice gap, 0 mm; flip angle, 90°; acquisition time, 1 min 13 s) and DTI with single shot EPI (TR, 10000 ms; TE, 60 ms; FOV, 300; matrix, 100×132, slice thickness, 3 mm; slice gap, 0 mm; SENSE factor, 2; b, 0–400 s/mm²; acquisition time, 6 min 12 s) images were acquired. Diffusion gradients were applied in 32 directions, and data were obtained at b values of 0 and 400 s/mm². For T1-weighted (T1W) IP and OP imaging, a T1 fast-field echo (FFE) sequence was used. The T1W IP, OP, and T2 TSE images were evaluated, and the signal intensity (SI) index was determined for each adrenal lesion. The total duration of the examination was approximately 18 min (range, 15–22 min).

DTI data analysis

Following data acquisition, all of the images were transferred to a manufacturer-supplied software system (PRIDE) for analysis. T2W TSE images were used for anatomical reference and for locating regions of interest (ROIs) on b=0 images, which were used to determine ADC and FA measurements. Lesions exhibiting possible cystic-necrotic components on T2W images were carefully avoided when inserting ROIs. Lesion characteristics on T2W images were examined by a radiologist experienced in body DWI image analysis. This radiologist was blinded to the findings from T1 IP and OP image analysis. Three measurements were obtained for each lesion, and the mean values of both ADC and FA were used for statistical analyses. The slice thickness, slice gap, and FOV values were identical for T2 and DTI sequences to ensure accurate anatomical correlation. Anisotropy and angular threshold values were in the range of 0.21–0.20 and 30–40, respectively. Color-coded FA maps were generated for each lesion. On these maps, blue represents the craniocaudal dimension of diffusion, red represents the medio-lateral dimension, and green represents the antero-posterior dimension. The color intensity corresponds to different strengths of anisotropy. A second radiologist evaluated the SI

index and the signal characteristics of the lesion images obtained with T1 and T2W sequences. This radiologist was blinded to the DTI findings and was experienced in body imaging.

Statistical analyses

The differences among the imaging parameters of adenomas and metastases were evaluated using a Mann-Whitney rank sum test. For multi-comparison corrections, the Bonferroni test was used. *P* values less than 0.05/6=0.008 were considered statistically significant. Spearman rank correlation analyses were performed to evaluate the correlations among FA, ADC changes in DTI images, and SI changes in T1 IP and OP images. *P* values less than 0.05/3=0.016 were considered statistically significant. In cases in which significant differences were detected in DTI parameters between adrenal adenomas and metastases, additional receiver operating characteristics (ROC) analyses were performed to determine the area under the curve (AUC).

Results

The age of the patients ranged from 45 to 73 years. The size of the lesions ranged from 10 to 64.6 mm, and their mean diameters were 24.8 mm for adenomas and 41.8 mm for metastases. Twenty-six of the lesions were located on the right side and seven were located on the left. The final diagnosis was adenoma for 19 of the lesions and metastases for the remaining 14.

The median FA value of the adrenal adenomas was 0.52, whereas the mean FA value of adrenal metastases was 0.35. The FA values of metastases were significantly lower than those of adenomas (*P* < 0.008). Based on ROC analysis, the AUC was found to be 0.936 for FA measurements with a 95% confidence interval. The cut-off value obtained from this analysis was 0.40 with maximum sensitivity and specificity values of 74% and 88%, respectively.

The median ADC value of adenomas was found to be 1.44 mm²/s, whereas the median ADC for metastases was 1.29 mm²/s. The median ADC value of metastases was lower than the median ADC value of adenomas, but this difference was not statistically significant. The median adrenal SI indices and ADC and FA values are displayed in Table 1. The T1 IP, OP, and

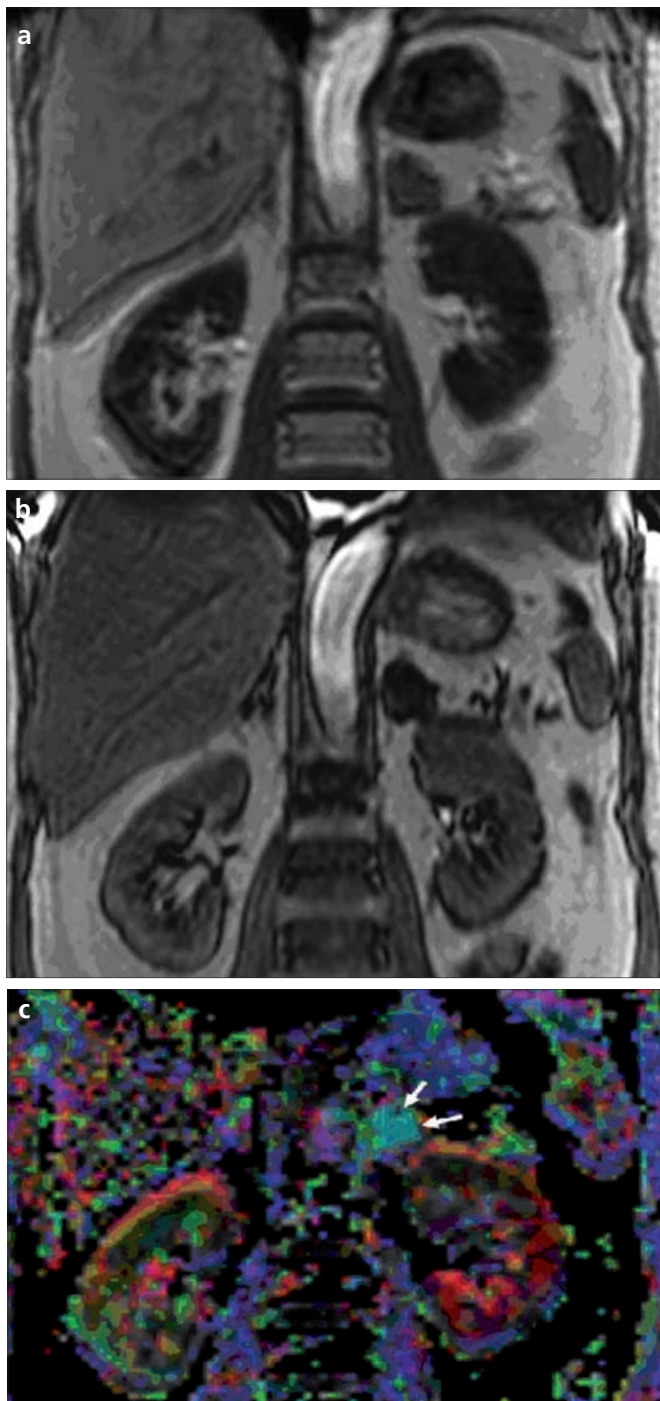


Figure 1. a–c. Coronal in-phase (a), opposed-phase (b), and color-coded fractional anisotropy map (c) images of a patient with adenoma (c, arrows).

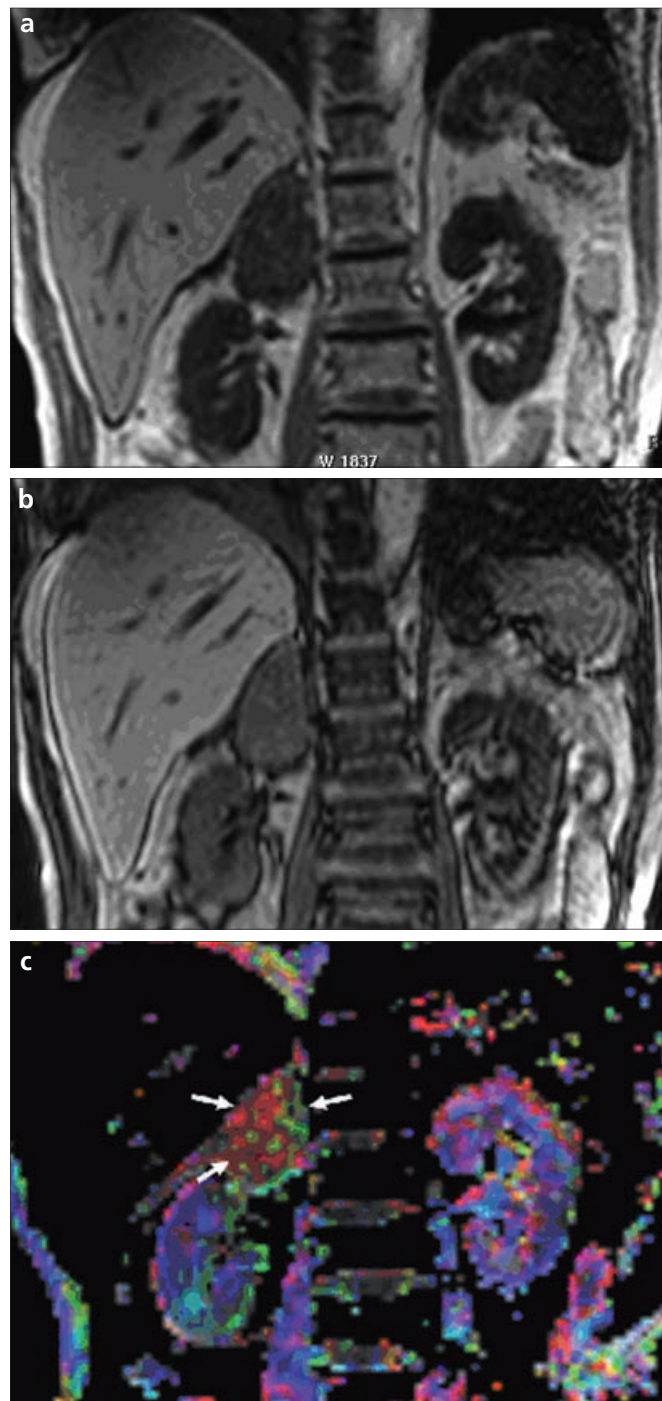


Figure 2. a–c. Coronal in-phase (a), opposed-phase (b), and color-coded fractional anisotropy map (c) images of a patient with metastases (c, arrows).

color-coded FA maps of two patients are also presented (Figs. 1 and 2).

A graph demonstrating the FAs and ADCs of adenoma and metastases is shown in Fig. 3, and a plot of these values is shown in Figs. 4 and 5.

The median SI indices for adenomas and metastases were 80.5 and 10.9, respectively. As expected, the adrenal SI indices obtained from T1W IP and OP

Table 1. The median signal intensity (SI) indices, fractional anisotropy (FA) values, and apparent diffusion coefficients (ADC) of adrenal adenomas and metastases

	SI index	FA	ADC
Adenomas	80.5	0.52	1.44
Metastases	10.9	0.35	1.29
<i>P</i>	0.001	0.001	0.454

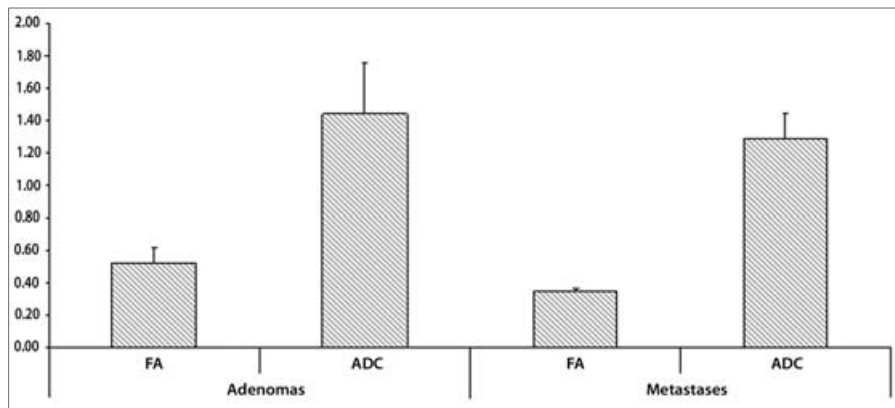


Figure 3. A bar graph displaying the fractional anisotropy (FA) values and apparent diffusion coefficients (ADC) of adrenal adenomas and metastases.

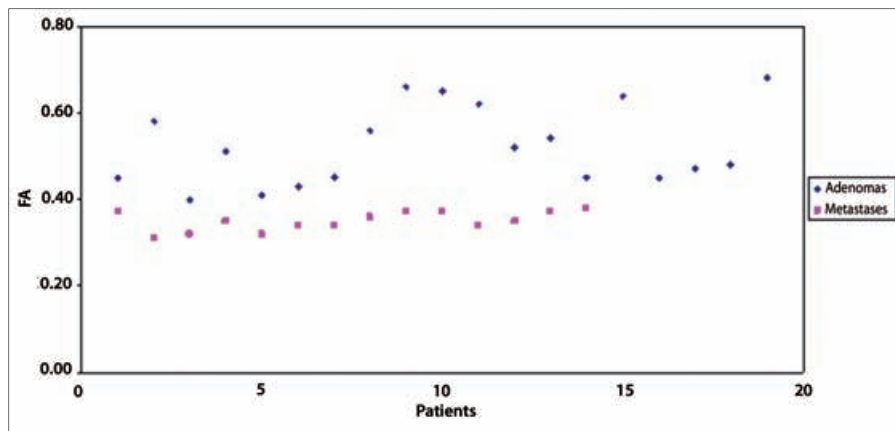


Figure 4. A plot of the fractional anisotropy (FA) values of all lesions.

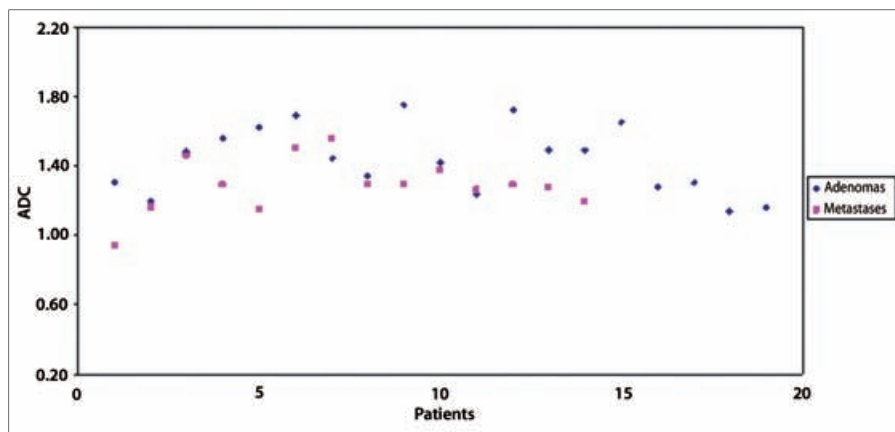


Figure 5. A plot of the apparent diffusion coefficients (ADC) of all lesions.

sequences were significantly higher for adenomas than those of metastases ($P < 0.001$).

There were no significant correlations between the differences in SI indices between the two lesion types and the measured DTI parameters (i.e., ADC and FA values).

Discussion

DWI is a non-invasive technique that provides both qualitative and quantitative data on tissue structures that can be used in the differential diagnosis of various pathological conditions. DWI data are principally derived from the thermally induced

motion of the hydrogen protons in water molecules, which is referred to as Brownian motion. In recent years, DWI has been integrated into a number of MRI examinations to aid in differential diagnosis. One of the most frequently used applications of DWI is oncological imaging. Generally, diffusion is restricted to a greater extent in solid tumor tissues than in non-tumoral tissues. As a result, tumoral tissue commonly exhibits high signal intensity on DWI and decreased ADCs. The greater restriction of diffusion in neoplastic cells has been attributed to increased amounts of membranes, cellular matrices, organelles, cytoskeletal components, and macromolecules (5, 6, 11, 12).

The use of DWI was initially only possible for neuroimaging applications. In parallel with technological advances, however, DWI and DTI examination of the abdominal viscera is now clinically feasible. There are two primary limitations in the application of DWI for body imaging: motion artifacts (e.g., respiratory, peristaltic) and the short T2 of the imaged organs, which necessitates a short TE. MRI systems with higher magnetic fields and improved signal-to-noise ratios have made it possible to perform DWI and DTI on the abdominal organs. The major obstacle for higher magnetic field systems is the associated increase in the susceptibility artifact. This difficulty can be overcome using parallel imaging technology, as described in this study. Parallel imaging techniques help to reduce the echo train length and the echo spacing (6, 12, 13).

It is important to note that diffusion is a multi-dimensional process, and the use of DWI alone may therefore result in a loss of important data on diffusion within highly organized (i.e., anisotropic) tissues. DTI is used to evaluate the anisotropic features of tissues and allows the analysis of diffusion in at least six different directions. This property of DTI enables the evaluation of anisotropy and provides more detailed data regarding the diffusion of water in various tissues (12, 14, 15). DWI and DTI have been used to examine a variety of intra-abdominal organs, including the liver, kidneys, and pelvic organs (7, 8, 12, 15). With respect to the adrenal gland, only DWI data have been

published (5, 11, 16). To the best of our knowledge, there has been no published study that employed DTI to study the adrenal glands. Miller et al. (5) used DWI to retrospectively evaluate 160 adrenal lesions with a wide variety of pathologies; they employed a 1.5 T MRI and parallel imaging technology and used three b values (0, 500, and 1000 s/mm²). A statistically significant difference was reported between the ADCs of cysts and other lesions. There was, however, no significant difference in ADCs between lipid-rich and lipid-poor adenomas or between benign and malignant lesions (5). Another DWI study of the adrenal glands was performed with a 1.5 T system and found that the ADCs of adenomas were significantly higher ($1.41 \pm 0.27 \times 10^{-3}$) than the ADCs of nonadenomatous solid lesions and cysts ($1.08 \pm 0.28 \times 10^{-3}$ and $2.82 \pm 0.24 \times 10^{-3}$, respectively) (16). Tsushima et al. (11) retrospectively investigated the DWI characteristics of adrenal adenomas (n=31), metastases (n=7), and pheochromocytomas (n=5) and found no significant difference between the ADCs of adenomas and metastases when using a 1.5 T scanner with two b values (0 and 1000 s/mm²). It is well established from DWI studies of tumors that benign lesions generally exhibit higher ADCs than do malignant lesions. Tsushima et al. (11) hypothesized that the absence of significantly high ADCs in adenomas compared with metastases may be the result of the densely packed cells of adrenal adenomas.

DTI has been used in many studies of the abdomen, including the prostate, liver, and kidneys. Feasibility studies of DTI in the kidney using 3 T MRIs have also been performed (12, 15, 17), and DTI has been shown to be beneficial in the differentiation of prostate cancer and chronic prostatitis (18). To the best of our knowledge, the adrenals have not previously been examined using DTI. In this study, we investigated the DTI parameters ADC and FA and their ability to differentiate adrenal adenomas from metastases. Although no significant difference was observed between adenomas and metastases with respect to ADCs, the mean FA value of adrenal adenomas was significantly higher than that of metastases. FA is a measure of the directional diffusivity of water and has a value between

0 and 1. In contrast to ADC data obtained using DWI, FA provides information regarding directional diffusion. We believe that FA may be more sensitive to some of the early ultrastructural tissue changes that occur before overt changes in the ADC occur. The differential sensitivity of FA and ADC with respect to tumor stage may explain the observed significant difference in the FA values of adenomas and metastases and the absence of a significant difference in the ADCs.

The standardization of DWI and DTI protocols is important for comparing and correlating results. The previously mentioned studies that performed DWI on the adrenal gland were performed with 1.5 T systems (5, 11, 16). Systems with higher magnetic fields offer benefits for DWI and DTI imaging. The increased signal-to-noise ratio in 3 T systems provides higher resolution and enables more accurate measurements of diffusion parameters with the same acquisition time as 1.5 T equipment. As a result, 3 T systems are preferable for DWI and DTI studies. Because this is the first study investigating the utility of DTI in the adrenal gland, it is not possible to compare our findings with those of other studies. However, the absence of a statistically significant difference in ADC parameters between adenoma and metastases is in agreement with the findings of Miller et al. (5) and Tsushima et al. (11). In addition to magnetic field strength, the b value is an important parameter that may affect diffusion parameters. When deciding the optimal b value for our study, we reviewed previous studies with b values ranging from 50 to 1000 s/mm². In these studies, the range of observed ADCs was between 0.85 and 2.82×10^{-3} (5, 11, 16). The optimal b value of a given tissue can be determined from the fact that $b \times \text{ADC}$ is equal to 1. ADCs within the range of previously reported values for adrenal lesions were inserted into this formula, resulting in b values between 350 and 1000 s/mm². This range appeared to be appropriate for adrenal DTI.

This study has a number of limitations; in particular, each of the adenomas included in this study displayed SI indices and signal characters suggestive of lipid-rich adenomas. Ideally, lipid-poor adenomas should also have been included in the study.

This modification to the study would necessitate biopsies from the subjects. The second major limitation is the limited number of patients.

In conclusion, this study demonstrates a significant difference in FA between adrenal adenomas and metastases. We believe that this finding may increase the diagnostic accuracy of MRIs when added to the routine protocol. Additional studies with larger patient groups that include lipid-poor adenomas are needed to test this hypothesis.

Conflict of interest disclosure

The authors declared no conflicts of interest.

References

1. Elsayes KM, Mukundan G, Narra VR, et al. Adrenal masses: MR imaging features with pathologic correlation. *Radiographics* 2004; 24:73–86.
2. Korobkin M, Lombardi TJ, Aisen AM, et al. Characterization of adrenal masses with chemical shift and gadolinium-enhanced MR imaging. *Radiology* 1995; 197:411–418.
3. Ctvrtlik, Herman M, Student V, Ticha V, Minarik J. Differential diagnosis of incidentally detected adrenal masses revealed on routine abdominal CT. *Eur J Radiol* 2009; 69:243–252.
4. Boland GW, Dwamena BA, Jagtiani Sangwaiya M, et al. Characterization of adrenal masses by using FDG PET: a systematic review and meta-analysis of diagnostic test performance. *Radiology* 2011; 259:117–126.
5. Miller FH, Wang Y, McCarthy RJ, et al. Utility of diffusion-weighted MRI in characterization of adrenal lesions. *AJR Am J Roentgenol* 2010; 194:179–185.
6. Bittencourt LK, Matos C, Coutinho AC Jr. Diffusion-weighted magnetic resonance imaging in the upper abdomen: technical issues and clinical applications. *Magn Reson Imaging Clin N Am* 2011; 19:111–131.
7. Chandarana H, Taouli B. Diffusion-weighted MRI and liver metastases. *Magn Reson Imaging Clin N Am* 2010; 18:451–464.
8. Notohamiprodo M, Reiser MF, Sourbron SP. Diffusion and perfusion of the kidney. *Eur J Radiol* 2010; 76:337–447.
9. Kartalis N, Lindholm TL, Aspelin P, Permert J, Albiin N. Diffusion-weighted magnetic resonance imaging of pancreas tumors. *Eur Radiol* 2009; 19:1981–1990.
10. Yamamura J, Salomon G, Buchert R, et al. Magnetic resonance imaging of prostate cancer: diffusion-weighted imaging in comparison with sextant biopsy. *J Comput Assist Tomogr* 2011; 35:223–228.
11. Tsushima Y, Takahashi-Taketomi A, Endo K. Diagnostic utility of diffusion-weighted MR imaging and apparent diffusion coefficient value for the diagnosis of adrenal tumors. *J Magn Reson Imaging* 2009; 29:112–117.

12. Gurses B, Kabakci N, Kovanlikaya A, et al. Diffusion tensor imaging of the normal prostate at 3 Tesla. *Eur Radiol* 2008; 18:716–721.
13. Rosenkrantz AB, Oei M, Babb JS, Niver BE, Taouli B. Diffusion-weighted imaging of the abdomen at 3 Tesla: image quality and apparent diffusion coefficient reproducibility compared with 1.5 Tesla. *J Magn Reson Imaging* 2011; 33:128–135.
14. Le Bihan D, Mangin JF, Poupon C, et al. Diffusion tensor imaging: concepts and applications. *J Magn Reson Imaging* 2001; 13:534–546.
15. Gurses B, Tasdelen N, Yencilek F, et al. Diagnostic utility of DTI in prostate cancer. *Eur J Radiol* 2011; 79:172–176.
16. Kilickesmez O, İnci E, Atilla S, et al. Diffusion-weighted imaging of the renal and adrenal lesions. *J Comput Assist Tomogr* 2009; 33:828–833.
17. Taouli B, Chouli M, Martin AJ, Qayyum A, Coakley FV, Vilgrain V. Chronic hepatitis: role of diffusion-weighted imaging and diffusion tensor imaging for the diagnosis of liver fibrosis and inflammation. *J Magn Reson Imaging* 2008; 28:89–95.
18. Gurses B, Kilickesmez O, Tasdelen N, Firat Z, Gurmen N. Diffusion tensor imaging of the kidney at 3 Tesla: normative values and repeatability of measurements in healthy volunteers. *Diagn Interv Radiol* 2011; 17:317–322.